Generation and Cyclic Remodeling of the Hair Follicle Immune System in Mice

Ralf Paus, Carina van der Veen, Stefan Eichmüller,[1] Tobias Kopp, Evelin Hagen, Sven Müller-Röver, and Udo Hofmann[1]

Department of Dermatology, Charité, Humboldt University, Berlin, Germany

In this immunohistomorphometric study, we have defined basic characteristics of the hair follicle (HF) immune system during follicle morphogenesis and cycling in C57BL/6 mice, in relation to the skin immune system. Langerhans cells and γδ T cell receptor immunoreactive lymphocytes were the predominant intraepithelial hematopoietic cells in neonatal mouse skin. After their numeric increase in the epidermis, these cells migrated into the HF, although only when follicle morphogenesis was almost completed. In contrast to Langerhans cells, γδ T cell receptor immunoreactive lymphocytes entered the HF only via the epidermis. Throughout HF morphogenesis and cycling, both cell types remained strikingly restricted to the distal outer root sheath. On extremely rare occasions, $CD4^+$ or $CD8^+$ αβTC were detected within the HF epithelium or the sebaceous gland. Major histocompatibility complex class II^+, MAC-1^+ cells of macrophage phenotype and numerous mast cells appeared very early on during HF development in the perifollicular dermis, and the percentage of degranulated mast cells significantly increased during the initiation of synchronized HF cycling (first catagen). During both depilation- and cyclosporine A-induced HF cycling, the numbers of intrafollicular Langerhans cells, γδ T cell receptor immunoreactive lymphocytes, and perifollicular dermal macrophages fluctuated significantly. Yet, no numeric increase of perifollicular macrophages was detectable during HF regression, questioning their proposed role in catagen induction. In summary, the HF immune system is generated fairly late during follicle development, shows striking differences to the extrafollicular skin immune system, and undergoes substantial hair cycle-associated remodeling. In addition, synchronized HF cycling is accompanied by profound alterations of the skin immune system. ***Key words: CD4/CD8/E cadherin/γδ T cells/hair cycle/integrins/MAC-1/NLDC145. J Invest Dermatol 111:7–18, 1998***

The hair follicle (HF) displays several intriguing immunologic features. For example, in striking contrast to the epidermis with its homogeneous distribution of intraepithelial lymphocytes, dendritic epidermal T cells (DETC) within murine HF epithelium are stringently restricted to a defined sector of the distal outer root sheath (ORS) (Paus *et al*, 1994a). Furthermore, the inner root sheath (IRS) and hair matrix of anagen follicles do not express major histocompatibility complex (MHC) class Ia molecules (Harrist *et al*, 1983; Westgate *et al*, 1991; Paus *et al*, 1994b) so that the proximal anagen follicle epithelium may enjoy some form of "immune privilege" (Billingham and Silvers, 1971; Westgate *et al*, 1991; Paus *et al*, 1994b, c; Paus, 1997). In addition, the distal ORS expresses so-called nonclassical MHC class Ib molecules (Paus *et al*, 1994b; Rückert *et al*, 1998).

Taken together, this has raised the possibility that the HF has a distinct "hair follicle immune system" (HIS) (Paus, 1997) that differs from the surrounding "skin immune system" (SIS) (Bos, 1997). Synchronized HF cycling is also associated with substantial alterations of the skin immune status and of standard skin immune responses (Claesson and Hardt, 1970; Westgate *et al*, 1991; Paus *et al*, 1994b; Hofmann *et al*, 1996, 1998; Tokura *et al*, 1997). In turn, the dermal SIS, namely mast cells (MC) and macrophages (MAC), may be involved in hair growth control (Parakkal, 1969; Westgate *et al*, 1991; Paus *et al*, 1994d; Botchkarev *et al*, 1995, 1997; Maurer *et al*, 1995, 1997).

Yet, even basic data on HF immunology are still missing. In particular, the following issues are still waiting to be clarified: (i) the migration of hematopoietic cells into the HF and the stepwise installation of the HIS during follicle morphogenesis, (ii) the exact distribution of Langerhans cells and αβ T cells throughout the entire HF epithelium, (iii) differences in the organization of the HIS during the hair cycle, and (iv) hair cycle-dependent changes in the number and distribution of extrafollicular constituents of the SIS, specifically of MAC.

To clarify these issues, we have studied the assembly of the HIS during neonatal HF morphogenesis in mice by standardized, quantitative immunohistomorphometry, using antibodies that demarcate γδ T cells, αβ T cells (CD4, CD8), Langerhans cells, MAC, and MC. With the exception of MC, which have already been extensively characterized (Paus *et al*, 1994d; Botchkarev *et al*, 1995, 1997; Maurer *et al*, 1997), the distribution and number of these immunocytes were also assessed during all stages of the hair cycle in adolescent mice, comparing pharmacologically and depilation-induced HF cycling.

Manuscript received April 24, 1997; revised February 19, 1998; accepted for publication February 26, 1998.

Reprint requests to: Dr. R. Paus, Department of Dermatology, Humboldt-Universität, Charité; Schumannstr. 20/21, D-10117 Berlin, Germany.

Abbreviations: CsA-HC, cyclosporine-induced hair cycle; dep-HC, depilation-induced hair cycle; γδTC, γδ T cell receptor-positive lymphocytes; γδTCR$^+$, γδ T-cell receptor immunoreactive; HF, hair follicle(s); HIS, hair follicle immune system; MAC, macrophages; MAC-1, CD11b (C3 bi receptor, = macrophage marker); MC, mast cells; MF, microscopic field; p.d., post-depilation; p.p., post-partum; SIS, skin immune system.

[1]Current address: Clinical Cooperation Unit for Dermato-Oncology (DKFZ), Department of Dermatology, University Hospital Mannheim, University of Heidelberg, D-68135 Mannheim, Germany.

Table I. Employed antibodies, source, and dilution

Antigen	Clone	Mainly expressed by	Source	Species	Dilution
pan-γδTCR	GL3[a]	γδ-receptor bearing T cells[i]	Pharmingen	hamster	1/75
CD4 (L3T4)	RM4–5	T helper lymphocytes,[i] MAC[j]	Pharmingen	rat	1/400
CD8 (Ly2)	53–6.7[b]	cytotoxic/suppresser T lymphocytes[i]	Pharmingen	rat	1/100
NLDC145	NLDC145[c]	Langerhans cells; dendritic cells[c]	BMA	rat	1/250
MAC-1 (CD11b)	M1/70[d]	MAC[d]	Pharmingen	rat	1/8000
MHC II	ER-TR3[e]	Langerhans cells (epidermis);[i] MAC, dermal dendritic cells[k]	BMA	rat	1/200
c-Kit	2B8[f]	MC, melanocytes[l]	Pharmingen	rat	1/200
E-cadherin	ECCD-1[g]	keratinocytes[m]	Zymed	rat	1/1500
$a^E/\beta 7$ (CD103)	m290[h]	intraepithelial T cells[n]	Pharmingen	rat	1/250

[a]Goodman and Lefrancois, 1989; [b]Ledbetter *et al*, 1980; [c]Kraal *et al*, 1986; [d]Springer *et al*, 1979; [e]van Vliet *et al*, 1984; [f]Ikuta and Weissman, 1992; [g]Yoshida-Noro *et al*, 1984; [h]Kilshaw and Murant, 1990; [i]Goldsmith, 1991; [j]Roulston *et al*, 1995; [k]Duraiswamy *et al*, 1994; [l]Hamann *et al*, 1995; [m]Hirai *et al*, 1989; [n]Lefrancois *et al*, 1994.

MATERIALS AND METHODS

Animals Tissue banks were prepared from neonatal and adolescent back skin of C57BL/6 mice obtained from Charles River (Sulzfeld, Germany) as described in detail (Paus *et al*, 1994e, 1997).

Induction of synchronized hair follicle cycling Anagen was induced by depilation of hair shafts on the back of mice with all follicles in telogen, as described (Paus *et al*, 1990, 1994f). In order to be able to distinguish changes in HF and skin immune parameters related to the trauma of depilation, which induces a discrete wound healing response early on during anagen development (Argyris, 1967), from truly hair cycling-related changes, a second, pharmacologic method of anagen induction was employed by i.p. application of cyclosporine A (CsA, Sandimmun; Sandoz, Basel, Switzerland). CsA was given once per day at a dosage of 250 mg per kg on days 0, 1, and 3, which initiates a new synchronized hair cycle (cyclosporine-induced hair cycle, CsA-HC) (Paus *et al*, 1989, 1996a). In both depilation- and CsA-induced anagen HF, catagen develops spontaneously after 17–19 d (Paus *et al*, 1994e, 1996a).

The time course of HF cycling after anagen induction by depilation (dep-HC) and after anagen induction by CsA (CsA-HC) were compared by quantitative histomorphometry (Paus *et al*, 1994e, 1996b; Maurer *et al*, 1997), analyzing 20 HF from each of five different mice during various time points of the dep-HC and the CsA-HC. This revealed that, in CsA-HC, anagen I was first detected 5 d after the first CsA injection, whereas anagen I could already be found at day 1 post-depilation (p.d.) in dep-HC. Thereafter the dynamics and time course of induced HF cycling were virtually identical between dep-HC and CsA-HC (data not shown). Thus, there is a time lap of 5 d between the onset of dep-HC and the onset of CsA-HC, after which both types of induced HF cycling show a practically identical anagen development.

Skin harvesting Back skin was dissected at the level of the subcutis just below the panniculus carnosus. For routine histology, paravertebral probes were taken from the upper half of the dissected skin and fixed in 5% buffered formalin, pH = 7.4. For immunohistology, skin probes from the lower half of the back skin were prepared for obtaining full longitudinal HF cryosections, using a special embedding technique (Paus *et al*, 1994a, b). In order to obtain samples of all stages of HF morphogenesis, neonatal mice were sacrificed on eight different days after birth [days 1, 3, 5, 7, 9, 11, 17, and 20 post-partum (p.p.)], whereas specimens of the dep-HC and CsA-HC were obtained on days 1, 3, 5, 8, 12, 17, 19, 25, and 34 p.d., or on days 4, 6, 8, 11, 15, 21, and 31 after the first CsA injection. These murine back skin samples with their well-defined hair cycle stages were compared with completely unmanipulated adolescent mouse skin with all HF in telogen (termed day 0) from 6 to 8 wk old C57BL/6 mice.

Histology The primary antibodies used for immunohistology and their source, dilution, and host species are listed in **Table I**. All incubation steps were interspersed by washing with Tris-buffered saline (TBS, 0.05 M, pH 7.6; 3 × 5 min). Non-specific binding was blocked by application of an avidin-biotin blocking kit solution (Vector Laboratories, Burlingame, VT) and by 5% bovine normal serum in TBS. Thereafter, sections were incubated with the primary antibody, diluted in TBS containing 1% bovine normal serum for 45 min (for dilution see **Table I**), followed by biotinylated secondary antibodies (goat anti-rat or rabbit anti-hamster, Dianova/Pharmingen; 1:200 in TBS containing 4% normal mouse serum; 30 min). Then the ABC-AP complex was added to the slides (Vector Laboratories; 1:100; 30 min), followed by staining for alkaline phosphatase, and counterstaining in Mayer's hemalaun (Handjiski *et al*, 1994). Double-labeling studies (see *Results*) were performed according to a method that we had developed for labeling skin sections with two primary antibodies from the same species (Eichmüller *et al*, 1996). Negative controls were obtained by omission of primary antibody, or by using nonspecific hamster or rat IgG instead. Because the expression of all tested antigens in one or all of these organs is well documented (e.g., Schuler, 1991; Janeway and Travers, 1997; Bos, 1997), thymus and spleen as well as murine skin itself served as positive controls. All control staining results for the employed primary antibodies yielded the expected immunoreactivity pattern (**Table I**). Giemsa staining was employed on paraffin-embedded longitudinal skin sections to identify MC by their characteristic morphology and the presence of metachromatic granules (Paus *et al*, 1994d).

Histomorphometry Based on functional and anatomical considerations, the epithelial and mesenchymal skin regions were divided into defined tissue compartments, as depicted in **Fig 1.** Twenty HF were analyzed for every mouse. Immunoreactive cells per epithelial compartment were counted after orienting a longitudinally cut HF into the center of the microscopic field [MF, ×400; strictly avoiding overlap of the interfollicular epidermal compartment (**Fig 1**, I)]. For evaluation of the mesenchymal compartments, a 31 μm wide strip (using an ocular micrometer grid) was virtually placed around the HF (**Fig 1**, compartments A, B, and C). During follicle morphogenesis, the dermal perifollicular mesenchyme (31 μm wide strip) was counted together as one "dermal compartment." Nine different stages of follicle morphogenesis (stages 0–8) can be distinguished in neonatal skin (Vielkind *et al*, 1995; Paus *et al*, 1997) (see *Results*). The compartment scheme for mature HF (**Fig 1**) was employed as soon as follicles had reached developmental stage 6 and later.

For the evaluation of mast cell numbers and degranulation patterns, all Giemsa-positive cells were counted within the perifollicular dermis and subcutis, and their granulation pattern was recorded ("not degranulated," no extracellular metachromatic granules visible; "strongly degranulated," > six extracellular mast cell granules). To evaluate the percentage of MHC II^+ cells among all dermal cells in telogen skin, and for comparing the absolute numbers of dermal MHC II/CD4 double-positive cells during telogen and anagen VI, a defined square reference area (0.015 mm^2) was randomly placed into the interfollicular dermis by the ocular micrometer grid (10 MF per mouse; five mice per day). Photomicrographs were taken with the Zeiss Axiophot system (Zeiss, Oberkochen, Germany). All immunoreactivity patterns were qualitatively recorded in standardized, computer-generated schemes of murine HF morphogenesis and cycling (Paus *et al*, 1997) by at least two independent observers.

Statistical analysis In neonatal mouse skin, a heterogeneous mixture of different stages of HF development is found during each of the first 7–8 d of life (Vielkind *et al*, 1995; Paus *et al*, 1997). Because our histomorphometric results were mostly obtained with reference to defined days of postnatal skin development, the prevalence of each stage of HF morphogenesis during each of these days was determined (i.e., on days 1, 3, 5, 7 p.p.; counting a total of 100 HF per day, i.e., 20 follicles each from five different mice). From this analysis, the percentage of follicles in late stages of follicle morphogenesis (stages 7 or 8) was calculated.

The mean cell numbers counted per compartment and mouse served as the basis for statistical analyses of immunocyte numbers. For each time point during neonatal follicle morphogenesis, dep-HC, or CsA-HC, and for each antigen, five mice (125 mice in total, >7500 HF) and 20 HF per mouse were analyzed. Statistical significance was estimated using the Kruskal–Wallis test for each compartment and – if positive – the Mann–Whitney U test for comparing pairs. For graphic representation, the mean and standard error of the mean as well as the p value were calculated.

RESULTS

During the early postnatal days, HF in very different stages of their development (e.g., **Fig 2*d***) were found located next to each other within the same skin section, representing tylotrich HF and the bulk

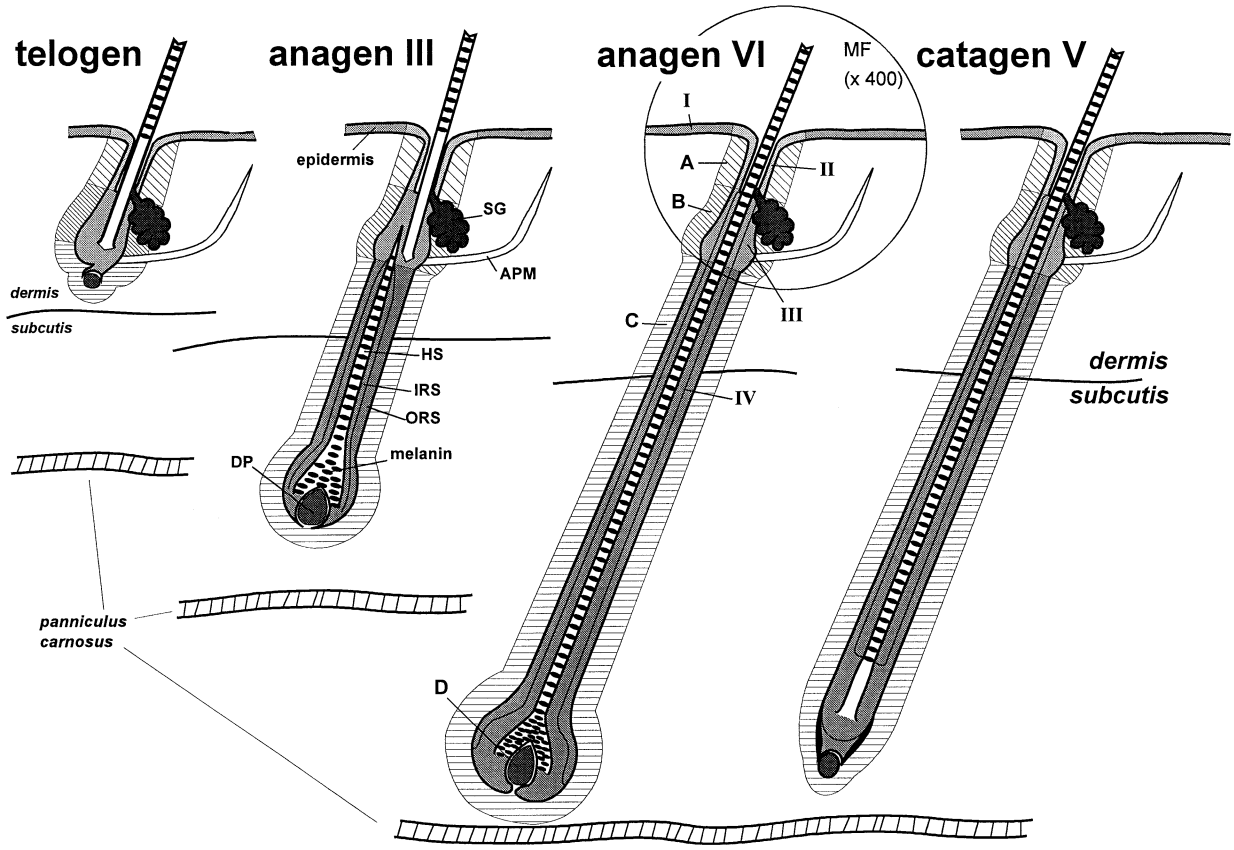

Figure 1. Defined epithelial and mesenchymal compartments of murine skin for quantitative immunohistomorphometry. The scheme depicts selected stages of hair follicle cycling and the corresponding changes of various C57BL/6 mouse skin and hair follicle compartments relative to each other. Epithelial compartments are in grey and roman numerals (I, epidermis; II, constant part of HF distal to sebaceous duct; III, isthmus and "bulge" region; IV, cycling part of HF; SG, sebaceous gland), and selected perifollicular mesenchymal compartments are hatched (A, B, C, perifollicular space; D, dermal papilla). Note the hair cycle-associated changes in the size of compartment C. For quantitative immunohistomorphometry, the microscopic field, here indicated in its starting position, was moved along the follicle and the numbers of immunoreactive cells in all compartments were counted and recorded (values for each compartment in **Figs 4–8** are given as the number of cells per MF). APM, arrector pili muscle; DP, dermal papilla; HS, hair shaft; IRS, inner root sheath; ORS, outer root sheath; SG, sebaceous gland.

of pelage follicles, which develop at various time points in the perinatal period (Vielkind *et al*, 1995; Paus *et al*, 1997). Because of this follicle heterogeneity, quantitative analyses were mostly performed with reference to selected days of neonatal skin development (see below). In addition, **Fig 3** qualitatively summarizes the obtained histomorphometric results on the distribution and relative numbers of γδ T cell receptor immunoreactive ($\gamma\delta TCR^+$) (DETC), NLDC-145^+ (Langerhans cells), MHC II^+ cells (Langerhans cells, MAC), and MC during defined stages of HF morphogenesis.

γδ T cell receptor-positive lymphocytes (γδTC) are the predominant immunocytes detectable in early postnatal epidermis Among immunocytes detectable during the first 7 d of neonatal life, γδ T cells were the first to populate the epidermis in substantial numbers (1–4 cells per MF, **Figs 2*a*, *f*, 4*a***). γδ T cell numbers continuously increased from day 1 p.p. to reach half-maximal numbers around days 4–5 p.p. (**Fig 4*a***), and their final density already at about day 7 p.p. (e.g., **Fig 2*f*, 4*a***). Interestingly, during days 1–2 p.p., directly adjacent "pairs" of $\gamma\delta TCR^+$ cells were frequently seen, whose phenotypic appearance suggested that these cells had just completed mitosis (cf. **Fig 2*a***) [DETC can proliferate intraepidermally during the perinatal period (Allison and Havran, 1991; Payer *et al*, 1991; Elbe *et al*, 1992)]. $\gamma\delta TCR^+$ cells were never seen in mesenchymal skin compartments.

Intraepithelial $CD4^+$ and $CD8^+$ T cells are most numerous in early neonatal epidermis Besides γδTC, a few $CD4^+$ αβ T cells (mean 0.4–0.5 cells per MF during days 1–7 p.p.; **Figs 4*b*, 5*a***) and even fewer $CD8^+$ αβ T cells (mean $<$ 0.2 cells per MF; **Fig 5*b***) could be detected in neonatal epidermis. There was a significant increase of epidermal $CD4^+$ cells from about 0.2 cells per MF on day 1 p.p. to a peak value of about one $CD4^+$ cell per MF on day 3 p.p., followed by a decline during the subsequent postnatal days (**Fig 4*b***). When comparing pooled data from mice during the early and the late neonatal period, the number of both $CD4^+$ and $CD8^+$ T cells in the epidermis declined with progressing skin and HF development (**Fig 5**).

$CD4^+$ T cells outnumber $CD8^+$ cells in neonatal mouse skin In the perifollicular dermis, the overwhelming majority of αβ T cells were $CD4^+$ T cells. Their numbers significantly increased during neonatal skin and HF development (**Fig 4*b*, 5*a***). $CD8^+$ cells instead were seen only extremely rarely in early neonatal dermis (0.01–0.02 cells per MF during days 1–7 p.p.), but substantially increased in number during subsequent postnatal days (**Fig 5*b***). Calculation of the CD4/CD8 ratios revealed that $CD4^+$ cells predominated over $CD8^+$ cells in both the epidermis (ratio: 3–5.8) and the dermis (ratio: 23–60) of neonatal C57BL/6 mouse skin.

The numeric increase of epidermal Langerhans cells in neonatal epidermis lags behind the one of γδTC In contrast to γδ T cells, we detected no NLDC-145^+ Langerhans cells and only very low numbers of MHC II^+ Langerhans cells in the epidermis during the first three postnatal days. Similar to a previous report (Elbe *et al*, 1989), Langerhans cells also displayed a steep numeric increase during progressing neonatal skin and HF development, with a short delay compared with DETC, to reach values of about three MHC II^+ and 5.5–6 NLDC 145^+ Langerhans cells per MF in the late postnatal phase. The half-maximal numbers of epidermal Langerhans cells were reached 2 or 3 d later than those of DETC, depending on the Langerhans cells marker employed (NLDC-145, MHC II; **Fig 4*a*, *c*, *d***).

Members of the dermal macrophage/dendritic cell lineage appear early in neonatal skin Already at day 1 p.p., prominent numbers of MHC II$^+$, NLDC-145$^+$, or MAC-1$^+$ subsets of the – still rather ill-defined – dermal dendritic cell populations of murine skin (Nickoloff, 1993; Bos, 1997) were found, scattered within the dermis and subcutis. Although the number of perifollicular dermal NLDC-145$^+$ cells, most likely representing Langerhans cells, remained very low during the first 20 d after birth (**Figs 2*g*, 4*c***), the number of perifollicular dermal MHC II$^+$ cells with macrophage-like phenotype continuously increased with progressing neonatal skin and HF development, reaching maximal levels at day 20 p.p. (**Figs 2*h*, 4*d***). In the perifollicular subcutis, only low numbers of MHC II$^+$ cells were seen (about 0.7 cells per MF on day 11 p.p., rising to 1.3 cells per MF on day 17 p.p.). MAC-1$^+$ cell populations could also be detected right after birth (**Fig 2*i***); they increased in number during the following days of skin and follicle morphogenesis much like what had been observed with MHC II$^+$ cells. Notably, compared with the more evenly distributed MHC II$^+$ cells, MAC-1$^+$ cells preferentially localized in the subcutis (not shown).

Mast cell activities change during hair follicle morphogenesis During early stages of murine neonatal skin and follicle development, MC were the most prominent hematopoietic cells to be found (**Fig 2*e***). Whereas the total number of dermal perifollicular MC changed only insignificantly during the first 17 d of postnatal life (range 2.2 to 3.5 cells per MF), HF development was paralleled by significant changes in the prevalence of degranulated MC. Between early postpartal days (days 3 or 5 p.p.) and days 9 and 11 p.p., i.e., when all follicles had developed into full-size anagen HF (**Fig 6*b***), a significant numeric increase of strongly degranulated perifollicular MC was detectable (**Fig 6*a***). The first catagen-telogen transformation (days 17–20 p.p.) was associated with a decline in the total MC number and in the number of nondegranulated MC (**Fig 6*a*, *b***), i.e., the initiation of synchronized HF cycling coincided with MC activation. This was confirmed when perifollicular MC were analyzed separately according

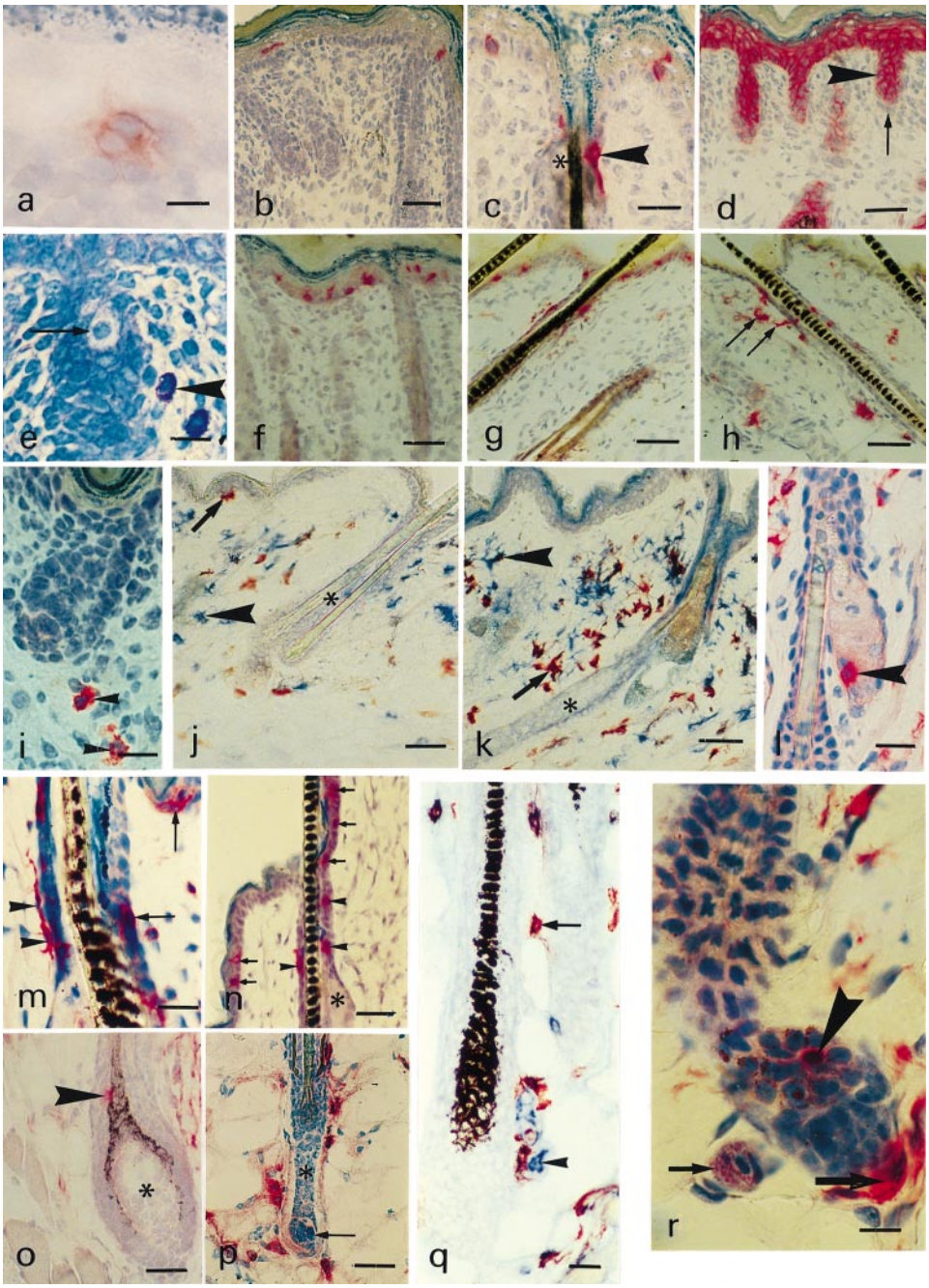

to the stage of follicle development (**Fig 6*c***), and by assessing MC by a degranulation-independent marker (c-Kit) (not shown).

The intrafollicular part of the HIS is assembled only during the final stages of HF morphogenesis During the first 7 d p.p., the dominant immunocyte populations of cutaneous epithelium, γδTC and Langerhans cells, were seen in notable numbers only within the epidermis (**Figs 2*a*, *b*, 3**) and in a minority of HF whose morphogenesis was already far advanced (e.g., **Fig 2*c***). These represented tylotrich follicles that had developed during late fetal life (Vielkind *et al*, 1995). Because the bulk of pelage HF all reached developmental stage 7 or 8 (**Fig 3**) around day 9 p.p. (**Figs 4*e*, 6*b***), and because γδTC and Langerhans cells almost always populated only those HF that had reached at least stage 7 of their morphogenesis (never before stage 6), the mean counts of intrafollicular γδTC and Langerhans cells significantly increased during this time period (**Fig 4*a*, *c*, *d***).

After the epidermal γδTC had reached their final density within the first 7 d p.p., this was followed by a significant numerical increase of intrafollicular γδTC, which became most obvious in compartment II around days 9–11 p.p. (**Fig 4*a***). Intrafollicular localization of $CD4^+$ or $CD8^+$ cells was an exceptionally rare event (mean < 0.06 cells per MF). Although these αβ T cells were present in relatively high numbers in the epidermis during the early neonatal phase (e.g., $CD4^+$ cells on day 3 p.p., one cell per MF; **Fig 4*b***), this did not result in any follicular increase of $CD4^+$ lymphocytes comparable with that of γδTC.

Immigration of NLDC-145^+ and/or MHC II^+ Langerhans cells into the HF started around the same time as that of γδTC, and resulted in comparable half-maximal settlement kinetics in the distal ORS (compartment II; **Figs 2*g*, *h*, 4*a*, *c*, *d***). Whereas γδTC obviously migrated into the follicle only via the epidermis (at the time of the intrafollicular increase in γδTC, no dermal $\gamma\delta TCR^+$ cells could be detected at all), Langerhans cells likely populated the follicle also via the distal perifollicular dermis (**Fig 2*h*, *m***) (the time point of rising numbers of intrafollicular Langerhans cells coincided with a significant numeric increase of perifollicular dermal Langerhans cells; see **Fig 4*c, d***).

E-cadherin and $\alpha^E/\beta7$-integrin (CD103) expression during HIS generation fail to explain follicular γδTC homing CD103, the heterotypic adhesion partner of E-cadherin, was found only on cells of dendritic phenotype within the epidermis and the distal follicle epithelium, corresponding exactly in number and distribution to the cells demarcated with the anti-γδTCR antibody (**Fig 2*b*, *c*, *f***; cf. Paus *et al*, 1994a). In contrast, E-cadherin was expressed on all keratinocytes of both the epidermis and the developing HF, independent of the HF stage (e.g., **Fig 2*d***). Thus, if the interaction of CD103 and E-cadherin plays any role in follicular T cell homing, comparable with the interaction of γδTC and epithelial cells in the intestinal mucosa (Cepek *et al*, 1994; Erle, 1995), it is most likely not a factor of primary importance and therefore does not explain the restricted distribution pattern of γδTC within the ORS.

Depilation-induced anagen development is associated with a numeric increase of immunocytes in most intra and perifollicular skin compartments Next we analyzed whether the synchronized cyclic growth and regression activity of mature HF in adolescent mice was associated with any changes in major cellular constituents of the HIS and/or the SIS. As shown in **Table II**, depilation-induced anagen development was indeed accompanied by a significant increase in the number of $\gamma\delta TCR^+$, NLDC-145^+, MHC II^+, or $CD8^+$ cells in a defined section of the distal ORS, and of MHC II^+, $CD4^+$, or $CD8^+$ cells in the proximal perifollicular mesenchyme. Notably, NLDC145^+, MHC II^+, or $\gamma\delta TCR^+$ cells were never seen to be localized within the distal inner root sheath or in the cycling part of the HF below the insertion of the arrector pili muscle (compartment IV), but were prominently represented in changing numbers within compartments I, II, or III. Interestingly, αβ T cells and NLDC-145^+ cells were rarely also detected in the outermost epithelial layer of the sebaceous gland (one example of a $CD4^+$ cell is shown in **Fig 2*l***). Thus, the intrafollicular distribution of all these immunocytes remained stringently restricted to the distal ORS throughout the hair cycle, as had been the case during follicle morphogenesis (**Fig 2*m*, *n***). In some skin compartments, the observed hair cycle-associated changes in immunocyte numbers differed between the dep-HC and the CsA-HC.

The previously reported, an anagen-associated increase in the number of epidermal γδ T cells during the dep-HC (Hashizume *et al*, 1994; Paus *et al*, 1994a) was not seen during CsA-HC (**Table II**). Though the number of NLDC-145^+ cells in the distal follicle epithelium significantly fluctuated between telogen and experimentally induced anagen VI, opposite, hair cycle-associated changes in the number of Langerhans cells were seen in the distal ORS, depending on whether dep-HC or CsA-HC was examined (see below). γδTC numbers in the most distal ORS (compartment II) of anagen VI follicles rose slightly over telogen values after hair cycle induction by depilation, but not after anagen induction by CsA. In compartment III, i.e., the isthmus and bulge region of the distal ORS, no significant changes in the γδTC number were detected (cf. **Table II**).

Figure 2. Photomicrographs of constituents of the HIS during hair follicle morphogenesis and cycling. Representative examples of the immunohistologic staining results obtained with the primary antibodies listed in **Table I** during various stages of HF and skin morphogenesis in neonatal C57BL/6 mice (*a–i*) and the depilation-induced hair cycle in adolescent C57BL/6 mice (*j–r*). (*a*) γδTCR: "pairs" of intraepidermal $\gamma\delta TCR^+$ lymphocytes, suggestive of mitosis, were frequently present at day 1 after birth (p.p.). (*b*) $\alpha^E/\beta7$ integrin (CD103): skin of neonatal mice at the first day after birth, showing a few, dendritic $CD103^+$ cells in the epidermis (most likely representing DETC) and two follicles of stage 3 on the right. (*c*) $\alpha^E/\beta7$ integrin (CD103): $CD103^+$ cells were visible already on day 4 p.p. within compartment II (*arrowhead*) of a developmentally advanced follicle [stage 7: tip of hair shaft has past the level where the sebaceous gland duct opens into the hair canal (*)]. (*d*) E-cadherin: at birth, epidermis and keratinocytes of HF buds (stage 2, *arrowhead*) were already strongly E $cadherin^+$; aggregated dermal papilla cells are visible directly below the follicle bud (*arrow*). (*e*) Mast cells (Giemsa): largely nondegranulated mast cell(s) (*arrowhead*) close to the distal part of a stage 5 follicle [note the single sebocyte (*arrow*) that characteristically becomes visible during this follicle morphogenesis stage] on day 1 p.p. (*f*) γδTCR: in the epidermis an increased density of $\gamma\delta TCR^+$ cells was detected at day 5 p.p., whereas $\gamma\delta TCR^+$ cells were still absent from the follicle epithelium at this time. (*g*) Langerhans cells: NLDC-145^+ Langerhans cells in epidermis and distal follicular ORS in the skin of mice on day 9 p.p. with all follicles in developmental stage 8. (*h*) Langerhans cells and MAC: MHC II^+ cells within epithelium and perifollicular dermis (*arrows*) of an early catagen follicle at day 18 p.p. (*i*) MAC: MAC-1^+ cells (*arrowheads*) in close vicinity of stage 3 hair follicle at day 1 p.p. (*j*) CD4/MHCII: CD4 (red, *arrow*)/MHC II (blue, *arrowhead*) double-staining of untreated telogen skin of adolescent mice showing a telogen follicle containing two club hairs (*), and numerous immunoreactive cells within the dermis. (*k*) CD4/MHCII: perifollicular dermal $CD4^+$ and MHC II^+ cells increase in both number and density during development of anagen VI (shown here exemplarily in anagen V skin; day 8 p.d.). (*l*) CD4: telogen HF, showing a $CD4^+$ T cell (*arrowhead*) within the outermost epithelial layer of the sebaceous gland (SG). γδTC or Langerhans cells were not found in the SG. (*m*) Langerhans cells: NLDC-145^+ cells within the epidermis and the HF (*arrows*), and in the perifollicular dermis (*arrowheads*) adjacent to the follicle epithelium of an anagen VI follicle (day 12 p.d.). (*n*) γδTC: typical distribution of $\gamma\delta TCR^+$ cells in distal ORS (*arrowheads*) of an anagen VI HF and in the epidermal epithelium (*arrows*). (*o*) CD4: the only T cells ever seen in the proximal HF epithelium (as an extremely rare phenomenon) were $\alpha\beta TCR^+$, $CD4^+$, or $CD8^+$ lymphocytes. Here, a $CD4^+$ T cell (*arrowhead*) is visible in the proximal ORS. Note the typical, expanded, voluminous dermal papilla (*) of an anagen HF, compared with the one of a telogen or a catagen HF (cf. *j*, *p*). (*p*) MAC-1: MAC adjacent to the prominent perifollicular connective tissue sheath and thickened basement membrane around a catagen VII follicle stained by anti-MAC-1 on day 19 p.d. At the proximal end of the epithelial strand (*) the typically rounded dermal papilla (*arrow*) of a late catagen follicle is seen. (*q*) MAC: during anagen VI MAC were often found in the direct vicinity of the proximal hair bulb, shown are blue MHC II^+ cells (*arrowhead*), red MAC-1^+ (*arrow*) cells, and purple double-labeled cells. (*r*) MHC II: an intrafollicular MHC II^+ cell (*arrowhead*) could only be detected in the regressing hair bulb on very rare occasions. The exceptionally rare phenomenon of an intraepithelial MHC II^+ cell in the hair germ of a catagen VIII HF on day 19 p.d. is shown here. The presence of additional $MHCII^+$ cells in the immediate vicinity (perifollicular connective tissue sheath, *large arrow*) suggests that the intrafollicular MHC II^+ cell is a MAC that has invaded the hair germ during the final stage of the catagen-telogen transformation. Note also the prominent perifollicular mast cell (*small arrow*). *Scale bars*: (*b, d, f, g, h, j, k, n, o, p, q*) 50 μm; (*c, e, i, l, m*) 25 μm; (*a, r*) 10 μm.

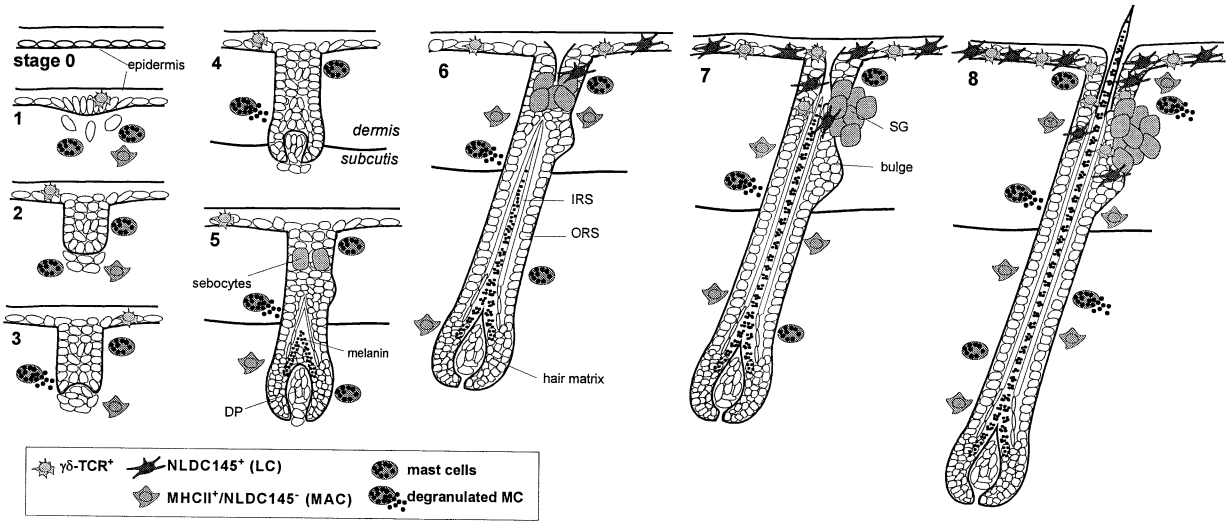

Figure 3. Hair follicle morphogenesis and stepwise generation of the HIS in neonatal mice. This schematic drawing shows the development of a HF in neonatal C57BL/6 mice and summarizes the arrangement of various constituents of the developing HIS. HF morphogenesis becomes morphologically visible at the placode stage (stage 1). By morphogenesis stage 8, the morphology of a mature, hair shaft-producing anagen VI follicle has been acquired (cf. **Fig 1**) (stages modified after Hardy, 1992). The HF only begins to cycle after that. As indicated, perifollicular MC and MAC can be found early on during follicle morphogenesis, whereas Langerhans cells and γδTC do not enter the follicle epithelium before stages 6–8 of development have been reached. DP, dermal papilla; IRS, inner root sheath; ORS, outer root sheath; SG, sebaceous gland.

$CD4^+$ and $CD8^+$ cells in adolescent skin and HF differ both in number and in localization Like in neonatal mice, the numbers of intraepithelial $CD4^+$ or $CD8^+$ cells in adolescent C57BL/6 mice were very low, and showed high degrees of interindividual variability between mice. Nevertheless, striking differences in αβ T cell numbers could be detected in defined skin compartments, when skin with all follicles in telogen or in induced anagen VI was compared; this also revealed substantial differences between neonatal and adolescent mouse skin (**Fig 5**).

Although the number of $CD4^+$ T cells in adolescent epidermis decreased to less than 0.1 cells per MF compared with 0.4 cells per MF in early neonatal epidermis, the distal follicle epithelium displayed rising numbers of $CD4^+$ cells during anagen development (**Fig 5*a***, **Table II**). Thus, telogen HF in adolescent mice had about the same equipment of $CD4^+$ T cells as the developing anagen follicles in early postnatal life, whereas anagen development in adolescent mice was characterized by a substantial influx (or local proliferation?) of these αβ T cells.

During both the dep-HC and the CsA-HC, the number of dermal $CD4^+$ cells, some of which may also represent MAC (Roulston *et al*, 1995; Wallgren *et al*, 1995), increased in anagen VI to about twice the telogen values (**Figs 2*j*, *k*, 5*a*, Table II**). Double-immunostaining for CD4 and MHC II antigens (**Fig 2*j*, *k***) was performed to distinguish dermal T cells from MAC, because $CD4^+$ T cells are generally MHC II negative (Janeway and Travers, 1997). This revealed that the absolute numbers of dermal MHC II and CD4 double-positive cells did not change significantly throughout the hair cycle (not shown), whereas that of dermal $CD4^+$ cells fluctuated significantly (**Fig 5**, **Table II**). Therefore, the anagen-associated increase in the number of dermal $CD4^+$ cells reflected an increase of this αβ T cell subset.

In adolescent mice, epidermal $CD8^+$ cells reached peak values of about 0.25 cells per MF during anagen VI. These were not significantly different from CD8 counts in telogen or early neonatal skin, but were significantly higher than those determined in late neonatal epidermis (about 0.03 $CD8^+$ cells per MF; **Fig 5*b***, **Table II**). As seen before with $CD4^+$ cells, anagen development in adolescent mice was associated with an increase in the number of intrafollicular $CD8^+$ cells, even though their total numbers remained very low throughout the hair cycle (**Fig 5*b***, **Table II**).

Interestingly, the epidermal CD4/CD8 ratio was lower than 1 throughout the adolescent depilation-induced hair cycle, reflecting a predominance of $CD8^+$ over $CD4^+$ T cells in adolescent epidermis. In contrast, $CD4^+$ cells dominated by far over $CD8^+$ cells, both in the HF and in the perifollicular dermis of adolescent mouse skin. The ratio of $CD4^+$ cells to $CD8^+$ cells basically did not change in any of the above skin compartments between telogen and anagen VI (not shown). The only T cells ever seen in the proximal HF epithelium, as an exceptionally rare phenomenon, were $CD4^+$ or $CD8^+$ lymphocytes (**Fig 2*o***).

Intraepithelial Langerhans cells numbers are hair cycle-dependent, but differ between dep-HC and CsA-HC In general, hair cycle-associated remodeling of the HIS and SIS was similar between dep-HC and CsA-HC (see **Table II**); however, in the epithelium differences between dep-HC and CsA-HC became apparent. Whereas MHC II and NLDC 145 antibodies demarcated significantly more epidermal Langerhans cells in anagen VI skin than in telogen skin during the CsA-HC, this was not seen during the dep-HC (**Table II**). In fact, we noted a significant anagen-associated decline of epidermal Langerhans cells during dep-HC, when NLDC-145 was used as a Langerhans cell marker (**Table II**). In the most distal ORS (compartment II), a significant, anagen-associated increase in the number of intrafollicular Langerhans cells above telogen values was found in dep-HC, whereas CsA-AVI showed a decrease (**Fig 2*m***; **Table II**). Using NLDC-145 as a Langerhans cell marker, significantly higher Langerhans cell numbers could also be detected in compartment III of dep-anagen VI compared with telogen HF (**Table II**), whereas the numbers during CsA-anagen were again lower.

NLDC-145 expression demarcates more intraepithelial Langerhans cells than MHC II expression Interestingly, using MHC II antigen expression for immunophenotyping, the maximal number of detected intraepithelial Langerhans cells was lower than when NLDC-145 was employed as the Langerhans cell marker in adolescent (**Table II**) or neonatal skin (**Fig 4*c*, *d***). Therefore, NLDC-145 antigen is a more sensitive immunohistologic marker for murine Langerhans cell detection *in situ* than MHC II. Whereas in nonactivated Langerhans cells the MHC II antigen is predominantly located in perinuclear patches and only weakly expressed on the cell surface, widespread NLDC-145 antigen expression is found on the Langerhans cell membrane (Schuler, 1991). This might explain the lower numbers of MHC II^+ cells detected in cryosections of murine skin, similar to the previously discussed differences in the anti-CD1 (an antigen that is also strongly expressed on the cell membrane) and anti-HLA-DR staining results of Langerhans cells in human skin (Schuler, 1991).

Dermal MHC II^+ cells are abundant in telogen skin and further increase during anagen development Besides numerous $CD4^+$

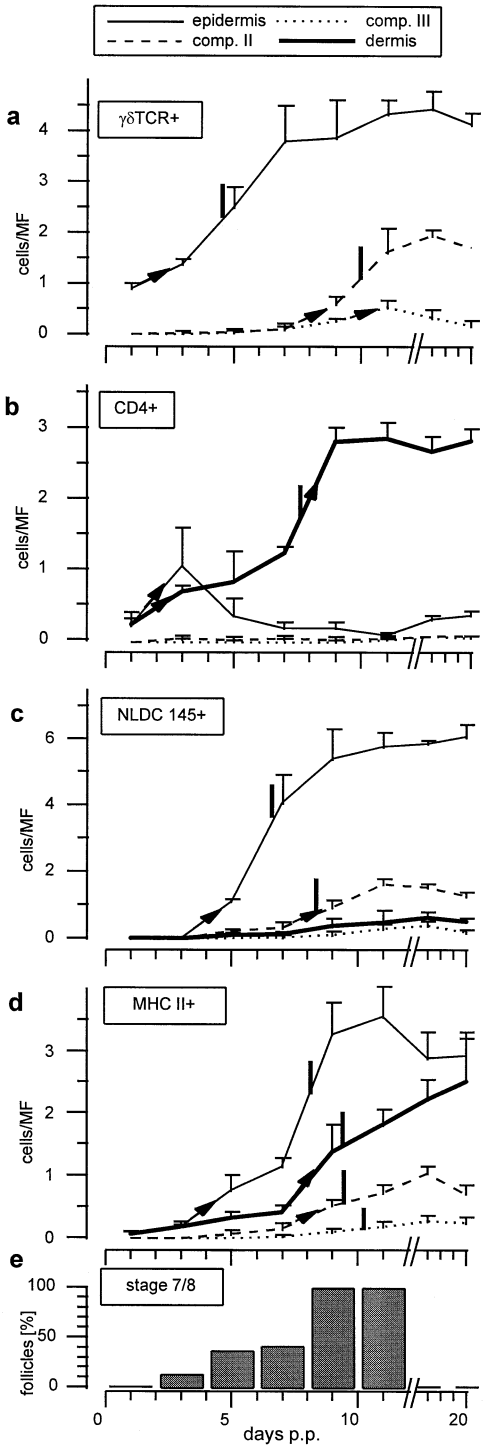

Figure 4. Quantitative analysis and distribution of $\gamma\delta TCR^+$ and $CD4^+$ lymphocytes, Langerhans cells, and MAC during neonatal hair follicle morphogenesis. (*a*) $\gamma\delta TCR^+$ cell numbers, (*b*) $CD4^+$ cell numbers, (*c*) NLDC-145^+ cell numbers (= Langerhans cells), and (*d*) MHC II^+ cell numbers (Langerhans cells in epidermis and compartments I + II, MAC in dermis) per MF; indicated as mean values ± SEM in defined compartments of the HF [epidermis, section of the interfollicular epidermis limited by the microscopic field, comp. II, ORS of HF distal to the sebaceous gland duct; comp. III, "bulge" region; dermis, sum of perifollicular compartments A + B (cf. **Fig 1**)]. *Black arrows* indicate the first significant increase of immunoreactive cells within a compartment within two consecutive days studied ($p < 0.05$); black bars indicate the time point when half-maximal numbers of immunoreactive cells are reached in the compartment. (*e*) Percentage of HF in stages 7 or 8 of follicle morphogenesis during the first 11 d p.p.

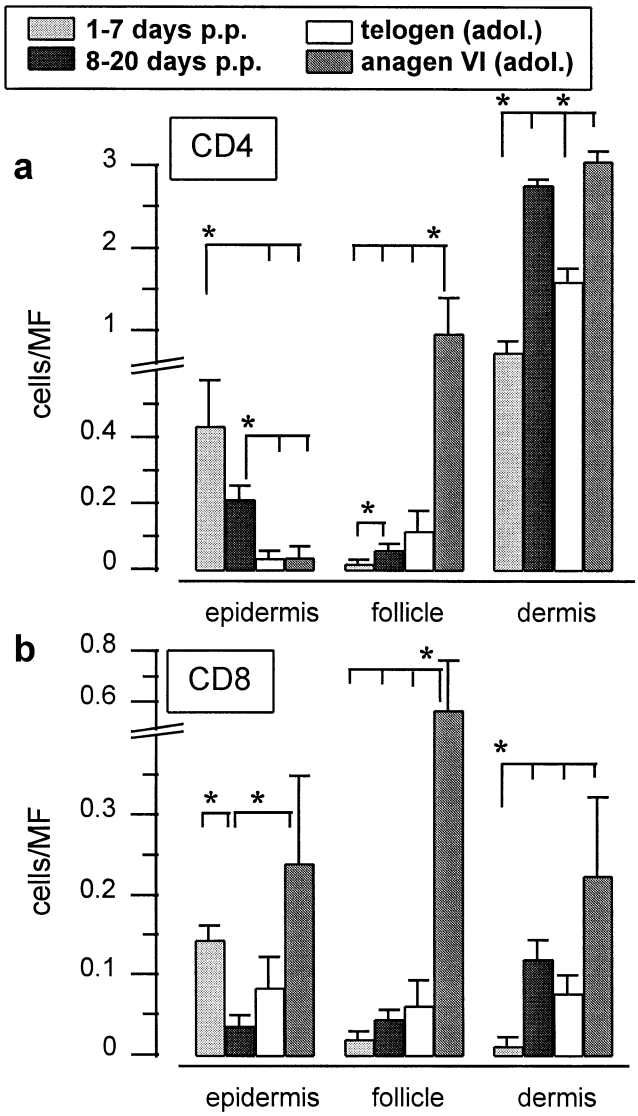

Figure 5. Dependence of the number and distribution of αβ T cells in murine skin on age and hair cycle phase. (*a*) $CD4^+$ cell numbers and (*b*) $CD8^+$ cell numbers. From all mice studied, the $CD4^+$ and $CD8^+$ cell numbers were determined for epidermis (compartment I), follicle epithelium (compartments II + III), and dermis (compartments A + B; cf. **Fig 1**). The data were pooled (indicated as mean values ± SEM) in four groups, distinguishing between two groups of early and late postnatal follicle development (days 1–7 p.p.; 8–20 p.p.), and by comparing data from telogen *versus* depilation-induced anagen VI in adolescent mice. *$p < 0.05$; neonatal groups: n = 20 mice, adolescent groups: n = 5 mice.

cells, the overwhelming majority of immunoreactive cells in the perifollicular mesenchyme were MHC II^+ cells, whereas only negligible numbers of NLDC-145^+ cells could be visualized in compartments A–C (cf. **Fig 1**) (< one cell per MF throughout the hair cycle; **Table II**). The MHC II-expressing cells were of dendritic shape within the dermis, or displayed a more rounded appearance in the comparatively loosely packed cellular environment of the subcutis (compare **Fig 2*j*, *k*, *q***). Quantitative immunohistomorphometry of unmanipulated adolescent telogen skin, surprisingly, revealed that not less than 30% of all nucleated interfollicular dermal cells *in situ* expressed MHC II antigen. This is a substantially higher value than the one previously reported by Duraiswamy *et al* (1994), who have determined an overall percentage of about 2.4% MHC II^+ cells among all cells in murine dermis (0.7% MAC-1 negative; 1.7% MAC-1 positive), using fluorescence-activated cell sorter analysis of dermal cell suspensions.

As shown in **Table II** and **Fig 7**, the number of perifollicular MHC II^+ cells within the perifollicular mesenchyme (A–C), increased highly

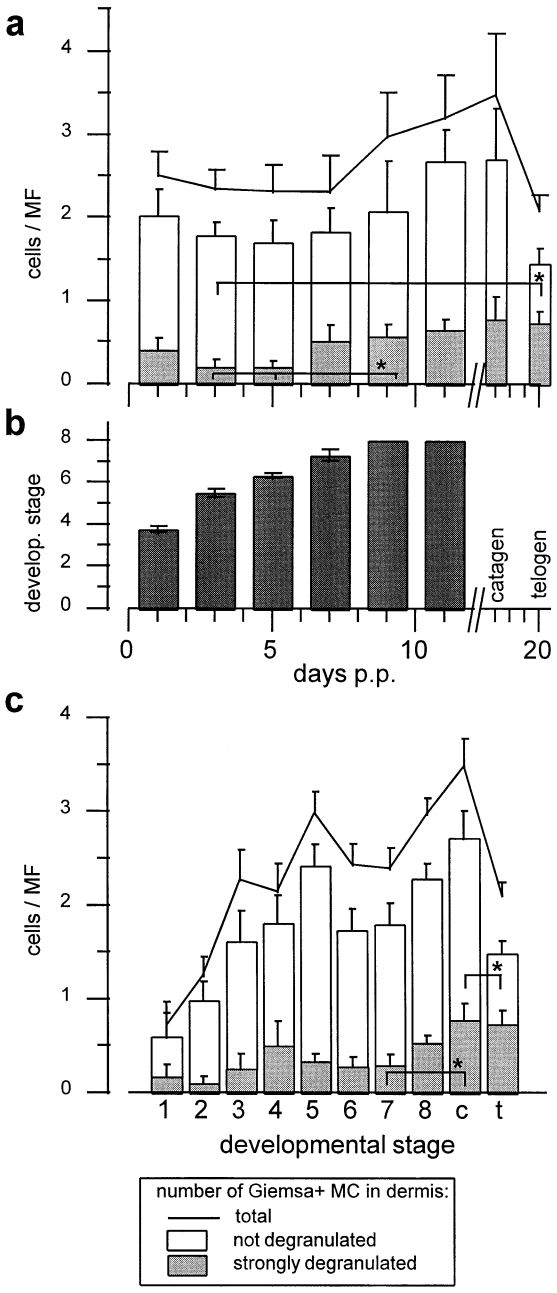

Figure 6. Numbers and degranulation pattern of perifollicular MC in neonatal skin. (*a*) Total numbers of dermal MC per MF distinguished between MC with signs of strong or absent degranulation. (*b*) Correlation with the progress in neonatal HF morphogenesis, expressed as the mean stage of follicle development reached at selected days p.p. (*c*) Numbers of perifollicular MC and their granulation status correlated with neonatal HF development. *$p < 0.05$, values are indicated as mean ± SEM; 20 follicles studied per mouse, n = 5 mice per day.

significantly during anagen development in both dep-HC and CsA-HC (**Fig 2*j*, *k***; **Table II**). Maximal numbers of macrophage-like MHC II^+ cells were counted around anagen V–VI follicles [days 8 and 12 p.d. (dep-HC) or days 12 and 15 after the first of three injections of CsA (CsA-HC)]. **Figure 7** also shows that the anagen-associated increase of perifollicular MHC II^+ cell numbers was long lasting (compartments A and B).

Although this was not evaluated quantitatively, MAC-1^+ cells in adolescent mouse skin were preferentially located in the perifollicular subcutis throughout the hair cycle, and showed a stronger immunoreactivity in this location than a population of more weakly stained MAC-1^+ cells in the dermis. Numbers and morphologic phenotype of MAC-1^+ and MHC II^+ cells were comparable with each other in the subcutaneous compartments (**Fig 2*p*, *q*, *r***).

The number of perifollicular MAC declines during catagen development During late anagen VI and the anagen-catagen transition, a significant decline in the number of perifollicular MHC II^+ cells was observed around the regressing hair bulb (compartment C, **Fig 7*c***). In addition, MAC-1^+ cells were counted and compared with MHC II^+ cell numbers at days 12 (anagen VI), 17 (anagen VI-early catagen), and 19 p.d. (late catagen; **Fig 8**). This revealed a significant decline of both MHC II and MAC-1^+ cells in the perifollicular mesenchyme during the anagen VI-catagen transformation even before the catagen-associated shrinkage of compartment C. Also, we never found any MHC class II^+ or MAC-1^+ cells to be located inside the regressing hair bulb epithelium during almost the entire anagen VI-catagen transformation of murine HF. Only in a single catagen VIII follicle among several hundred screened follicles in various stages of catagen development, i.e., at the very end of catagen development, did we note an intraepithelial MHC class II^+ cell inside the regressing hair germ, surrounded by several MHC class II^+, macrophage-like cells in the directly adjacent perifollicular connective tissue sheath (**Fig 2*r***).

DISCUSSION

This study complements previous work on murine HF immunology (e.g., Hashizume *et al*, 1994; Paus *et al*, 1994a, b, d, 1996a; Botchkarev *et al*, 1995, 1997; Hofmann *et al*, 1996, 1998; Slominski *et al*, 1997; Tokura *et al*, 1997), and closes important gaps of knowledge in the emerging field of "trichoimmunology" (Paus, 1997) by characterizing (i) the migration of hematopoietic cells into the murine HF during its morphogenesis, (ii) the exact intrafollicular distribution of antigen presenting cells and αβ T cells, (iii) hair cycle-dependent changes in the organization of the HIS, and (iv) changes in the number and distribution of selected perifollicular constituents of the SIS during HF development and cycling. Several new insights and concepts surface from this basic phenomenologic study.

The murine HIS is composed of selected components of the SIS, namely of *intrafollicular* Langerhans cells and γδTC, located exclusively in the distal ORS (**Figs 2*c*, *g*, *h*, *m*, *n*, 3**), as well as by a unique follicular MHC class I-, adhesion molecule-, and extracellular matrix-expression pattern (see below), and by *perifollicular* MC and MAC populations (**Figs 2*e*, *h*, *i*, *p*, *q*, *r*, 3**). Due to their extremely low number, intrafollicular $CD4^+$ or $CD8^+$ αβ T cells probably do not play an important role in the normal murine HIS. During follicle morphogenesis, this HIS is assembled stepwise, beginning with its perifollicular components: MAC-1^+ MAC and MC are the first cells to appear around the developing follicle buds, which remain devoid of γδTC and Langerhans cells until follicle morphogenesis has almost been completed (**Fig 3**).

Langerhans cells and γδTC migrate into the follicle epithelium only after follicle morphogenesis is far advanced (stages 6–8), and then remain restricted throughout all stages of subsequent HF cycling to the ORS above the insertion of the arrector pili muscle, including the bulge (i.e., stem cell) region (**Figs 2*g*, *h*, *m*, *n*, 3**). Langerhans cells and γδTC populate the follicle at the earliest when the sebaceous gland duct is formed, and at the latest by the time the hair shaft begins to penetrate the epidermis (**Figs 2*c*, *g*, *h*, 3**). This suggests that the HIS begins to form only when the construction of follicular canal and sebaceous gland duct opens major ports of entry for microbial invasion into the mammalian organism. Because γδTC lines have been identified that can interact with Langerhans cells *in vitro* (Porcelli *et al*, 1989; Haas *et al*, 1993), and because some γδTC populations can recognize conserved bacterial antigens presented to them by MHC class Ib molecules like Qa-2 (Rötzschke *et al*, 1993; Shawar *et al*, 1994; Melian *et al*, 1996), which are strongly expressed only in the distal follicle epithelium (Paus *et al*, 1994b; Rückert *et al*, 1998), it is conceivable that intrafollicular γδTC, Langerhans cells, and MHC class Ib molecules interact in the context of the HIS. This may serve to generate a phylogenetically ancient, regional intraepithelial "anti-infection defense" and "trauma surveillance" meshwork of interacting dendritic cells and MHC class Ib-expressing keratinocytes, which protects the

Table II. Changes in the number of immunocytes visualized in defined compartments of C57BL/6 mouse back skin with all hair follicles in telogen or induced anagen VI[a]

		I	II	III	A	B	C
γδTCR	T	3.72 ± 0.27	1.62 ± 0.11	0.37 ± 0.13	0	0	0
	Dep AVI	6.21 ± 0.33 ↑↑	2.41 ± 0.18 ↑	0.12 ± 0.05 ns	0	0	0
	CsA AVI	**3.48 ± 0.24** ns	1.71 ± 0.19 ns	0.22 ± 0.05 ns	0	0	0
NLDC145	T	5.04 ± 0.15	2.10 ± 0.15	0.87 ± 0.06	0.34 ± 0.07	0.28 ± 0.07	0.09 ± 0.06
	Dep AVI	3.98 ± 0.12 ↓↓	2.89 ± 0.09 ↑↑	1.49 ± 0.06 ↑↑	0.36 ± 0.07 ns	0.32 ± 0.06 ns	0.13 ± 0.05 ns
	CsA AVI	**6.50 ± 0.38** ↑↑	**1.19 ± 0.08** ↓↓	**0.58 ± 0.09** ↓	0.57 ± 0.12 ns	0.21 ± 0.03 ns	0.30 ± 0.09 ns
MHC II	T	3.36 ± 0.66	1.23 ± 0.19	0.66 ± 0.12	2.26 ± 0.26	1.73 ± 0.15	2.71 ± 0.43
	Dep AVI	3.32 ± 0.27 ns	2.10 ± 0.26 ↑	0.65 ± 0.14 ns	4.10 ± 0.43 ↑	3.68 ± 0.39 ↑↑	13.02 ± 0.91 ↑↑
	CsA AVI	**5.35 ± 0.27** ↑	**0.93 ± 0.05** ns	0.50 ± 0.04 ns	4.83 ± 0.32 ↑↑	4.63 ± 0.15 ↑↑	**7.54 ± 0.52** ↑↑
CD4	T	0.04 ± 0.02	0.06 ± 0.03	0.06 ± 0.04	0.74 ± 0.08	0.86 ± 0.10	0.88 ± 0.03
	Dep AVI	0.04 ± 0.03 ns	0.36 ± 0.14 ns	0.61 ± 0.30 ↑↑	1.31 ± 0.14 ↑	1.75 ± 0.09 ↑↑	1.53 ± 0.09 ↑↑
	CsA AVI	**0.34 ± 0.04** ↑↑	0.12 ± 0.05 ns	0.22 ± 0.05 ↑	1.29 ± 0.23 ns	1.40 ± 0.03 ↑↑	1.72 ± 0.22 ↑↑
CD8	T	0.09 ± 0.04	0.05 ± 0.02	0.01 ± 0.01	0.03 ± 0.01	0.05 ± 0.03	0.21 ± 0.05
	Dep AVI	0.24 ± 0.11 ns	0.37 ± 0.14 ↑	0.21 ± 0.08 ↑	0.13 ± 0.06 ↑	0.10 ± 0.04 ns	0.57 ± 0.15 ↑
	CsA AVI	0.18 ± 0.07 ns	0.09 ± 0.03 ns	0.09 ± 0.05 ns	0.15 ± 0.03 ↑↑	0.28 ± 0.04 ↑	0.44 ± 0.09 ↑

[a]The number of immunoreactive cells per compartment and MF was counted in 8 μm thick sections, and is given as the mean ± SEM (assessing 20 MF from five mice per hair cycle stage), including both dep-HC and CsA-HC. ↑, ↓, $p < 0.05$; ↑↑, ↓↓, $p < 0.01$, for statistically significant differences between telogen and either Dep AVI or CsA AVI. Statistically significant differences between Dep AVI and CsA AVI are indicated by underlined, bold figures ($p < 0.01$). The location and extension of each histomorphometry compartment is explained in **Fig 1**. Dep AVI, anagen VI HF from dep-HC; CsA AVI, anagen VI HF from CsA-HC.

follicle region most exposed and most vulnerable to infection and trauma (Paus *et al*, 1994b; Paus, 1997; Rückert *et al*, 1998). Thus, by the time the follicular canal gets populated by a rich, commensural microbial flora (Noble, 1993), this flora already meets with all cellular constituents of the HIS in their definitive intrafollicular positions.

The mechanisms that dictate the stringent distribution pattern of γδTC and Langerhans cells (i.e., the specifics of the local adhesion and cytokine milieu of the distal ORS) remain to be characterized. Our data suggest that at least one major recognized homing mechanism for intraepithelial T cells, heterotypic interactions between E-cadherin expressed on epithelial cells and $\alpha^E/\beta 7$ integrin on T cells (Cepek *et al*, 1994; Erle, 1995), is probably not of primary importance in follicular γδTC homing. Whereas γδTC enter the distal follicle epithelium via the epidermis, Langerhans cells appear to do so via the surrounding dermis (**Fig 2*h*, *m***). This suggests the existence of distinct follicular homing mechanisms for Langerhans cells and γδTC.

γδTC become visible in the epidermis long before they migrate into the follicle (**Fig 2*a*, *b*, *f***). In fact, γδTC may first have to enter the epidermis in order to proliferate (Payer *et al*, 1991; Elbe *et al*, 1992) (cf. **Fig 2*a***) and/or to mature in an appropriate cytokine and adhesion milieu (Bergstresser *et al*, 1993; Tigelaar and Lewis, 1995) provided only by the neonatal epidermis, until the γδTC population has been sufficiently expanded for export into the follicle. Intraepidermal and intrafollicular γδTC most probably arise from the same precursor cells, because they express the same TCR Vγ3/δ1 subtype (Paus *et al*, 1994a). Because a special affinity of DETC for anagen HF has been reported (Tigelaar and Lewis, 1995), it is noteworthy that epidermal γδTC do not enter the developing HF until it is almost indistinguishable from a mature anagen follicle (**Figs 2*c*, *f*, 3**). This may reflect that only the distal epithelium of anagen HF generates an appropriate cytokine and/or adhesion milieu for these γδTC, which may resemble that provided by the neonatal epidermis.

Among the hematopoietic cells investigated here, MAC and MC are the first ones to appear in prominent numbers in the perifollicular dermis during early neonatal skin and HF development (**Figs 2*e*, *i*, 3**). Although MC and MAC are traditionally viewed as chief representatives of innate immunity (Janeway and Travers, 1997; Bos, 1997), they may also play an important role during HF cycling in later life (Parakkal, 1969; Westgate *et al*, 1991; Paus *et al*, 1994d; Maurer *et al*, 1995, 1997). It is therefore interesting to ask whether these cells also contribute to the control of HF morphogenesis, and whether factors secreted by the developing follicle epithelium attract MC and MAC to enter the dermis and/or induce them to mature here so that they become identifiable by standard markers. Increasing evidence supports the hypothesis that MC degranulation, at least in mice, is involved not only in modulating the telogen-anagen transformation, but also in catagen development (Paus *et al*, 1994d; Maurer *et al*, 1997). Thus, it is conceivable that the activation/degranulation of selected MC populations during the final stage of neonatal HF development revealed here (**Fig 6**) contributes to the first synchronized catagen transformation of the newly formed HF.

Contrary to a recent report (Tamaki *et al*, 1996), we did not detect any γδTC in neonatal or adolescent mouse dermis (using a pan-γδTCR antibody and conventional immunohistology), where only αβ T cells could be identified (**Fig 2*j*, *k***). In murine epidermis and HF epithelium, αβ T cells are seen only very rarely; however, in contrast to γδTC, they are also found in the outermost epithelial layer of the sebaceous gland (**Fig 2*l***). Throughout normal murine skin of all ages, the few detectable $CD4^+$ outnumber by far the $CD8^+$ T cells (**Fig 5**), yet, the predominance of $CD4^+$ over $CD8^+$ T cells differs between distal follicle epithelium, dermis, and epidermis (see *Results*). This may reflect that follicle epithelium, epidermis, and dermis each provide a distinct homing milieu for $CD4^+$ and $CD8^+$ T cells.

As a very rare event, a single $CD4^+$ T cell could be seen in the follicle epithelium even below the bulge (**Fig 2*o***), i.e., in an intraepithelial territory devoid of γδTC and Langerhans cells. Therefore, the intrafollicular distribution of "trafficking" αβ T cells (Bos, 1997) is less restricted than that of reputedly rather "sessile" epidermal γδTC (Tigelaar *et al*, 1991; Bergstresser *et al*, 1993). Thus, the "immunoprivileged" anagen hair bulb (Billingham and Silvers, 1971; Westgate *et al*, 1991; Paus, 1997), in principle, may still be accessible to αβ T cells. This may be important to understand how this immune privilege may collapse in the context of inflammatory hair growth disorders like alopecia areata (Paus *et al*, 1994c; Becker *et al*, 1996).

As previously shown for MC (Paus *et al*, 1994d; Botchkarev *et al*, 1995; Maurer *et al*, 1995, 1997), the number of perifollicular MAC also changes during both the dep-HC and the CsA-HC, with maximal numbers of perifollicular, $MHC\ II^+$/NLDC-145-negative MAC-like populations detectable in synchronized anagen V–VI (**Table II**; **Figs 2*q*, 8**). The number of dermal $CD4^+$ T cells, a minority of which may represent MAC, increases similarly impressively during synchronized anagen development (**Figs 2*j*, *k*, 4, 5*a***). Thus, the extrafollicular components of the HIS are also continuously remodeled during HF cycling. Although the functional significance of this observation remains to be elucidated, this underlines once more the critical importance of considering and standardizing the hair cycle stage of the integument during immunologic analyses in mice (Hofmann *et al*, 1996, 1998; Paus, 1997; Slominski *et al*, 1997; Tokura *et al*, 1997).

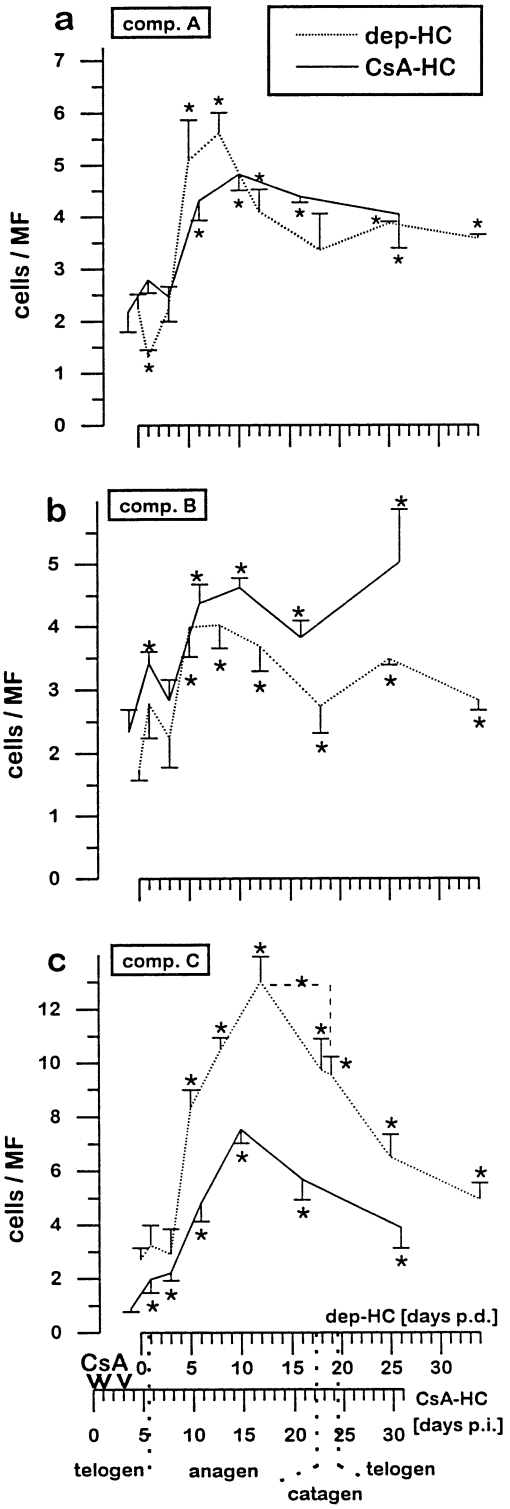

Figure 7. Perifollicular MHC II$^+$ cells during the adolescent hair cycle. A prominent anagen-associated increase in all perifollicular compartments A (*a*), B (*b*), and C (*c*) (cf. **Fig 1**) was observed during both types of hair cycle induction. Note the rising cell numbers in compartments A and B whose size remains fairly constant during the hair cycle. *Significant difference to telogen values or to values connected by bracket; $p < 0.05$; values are indicated as mean ± SEM. days p.i., days after inspection of cyclosporin A (CsA).

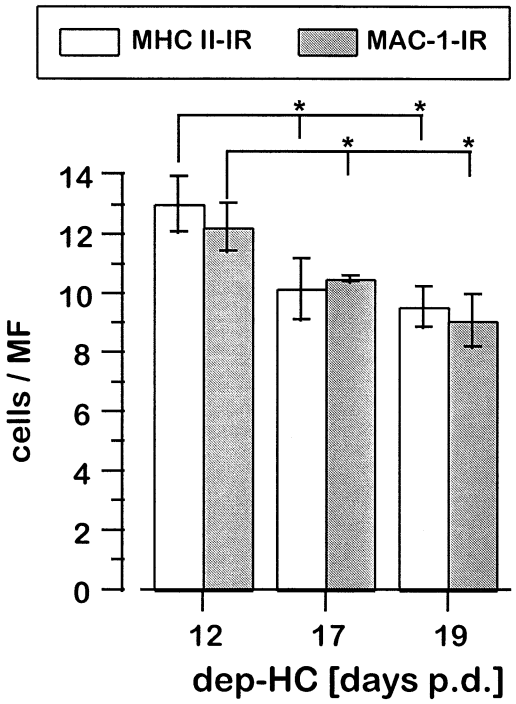

Figure 8. Numbers of perifollicular MAC-1$^+$ and MHC II$^+$ cells during the anagen–catagen transformation of HF. MHC II and MAC-1 expression served as markers for characterizing the numbers of dermal/subcutaneous perifollicular MAC/phagocytes in compartment C, i.e., in the direct vicinity of the spontaneously regressing hair bulb (cf. **Fig 1**) during day 12 (anagen VI), day 17 (early catagen), and day 19 (mid-late catagen) after depilation. *Significant difference to values obtained in anagen VI ($p < 0.05$); values are indicated as mean ± SEM from analysing five mice per time point. Note that there is no increase in the number of MAC-1$^+$ cells with the phenotypic appearance of MAC around the regressing hair bulb and that, in fact, their numbers decline during the anagen VI–catagen transformation.

It has been proposed that catagen development is functionally linked to MAC attacking the regressing hair bulb (Westgate *et al*, 1991). No MAC, however, can be seen to invade the follicle epithelium during the anagen VI to catagen VII transformation in mice, and there is no increase in the number of perifollicular MAC during catagen development (if anything, their number even declines! cf. **Fig 8**). Thus, it appears unlikely that MAC are critically involved in murine catagen induction.

Only a systematic comparison with spontaneous HF cycling, which is under preparation in our laboratory, will clarify to what extend the observed hair cycle-dependent fluctuations in extra- and intrafollicular immunocytes may represent experimental artifacts related to depilation or CsA administration. There are indeed interesting differences between dep-HC and CsA-HC, which suggest that the method of hair cycle induction also determines how the HIS is remodeled during anagen development. For example, whereas the number of Langerhans cells in the distal ORS of anagen VI HF rises above that of telogen HF, CsA-induced anagen VI HF actually shows a numeric decrease of Langerhans cells in this HF region (**Table II**). In contrast, the number of perifollicular MAC shows highly comparable hair cycle-dependent changes between dep-HC and CsA-HC (**Table II**, **Fig 7**). Thus, currently at least the anagen-associated increase in perifollicular MAC numbers can safely be assumed to be truly hair cycle-related, independent of the method of anagen induction.

The differences in the number of intraepidermal Langerhans cells between dep-HC and CsA-HC were particularly unexpected. During the CsA-HC, significantly more MHC II$^+$ epidermal Langerhans cells were detected in anagen VI skin than in telogen skin; no such anagen-associated increase in MHC II$^+$ cells with dendritic morphology was apparent in the epidermis of dep-HC (**Table II**). Using NLDC 145 as a Langerhans cell marker, there was even a slight, but significant anagen-associated decline of NLDC 145$^+$ epidermal Langerhans cells during dep-HC, whereas NLDC 145$^+$ Langerhans cells slightly increased in number during the CsA-HC (**Table II**). An analysis of these interesting differences in MHC II and NLDC 145 expression by epidermal Langerhans cells is beyond the scope of this study, because

they pertain more to epidermal Langerhans cells biology in general than to the biology of the HIS. These differences, however, pose intriguing questions as to how MHC II- and NLDC 145 (co)expression by epidermal Langerhans cells is controlled (Schuler, 1991; Bos, 1997), and as to how various Langerhans cell populations in murine skin epithelium differ from each other, e.g., in their response to trauma (depilation) and immunosuppression (CsA).

The presented immuno-histomorphometric data on the generation and remodeling of the murine HIS during HF morphogenesis and cycling pave the way for the functional studies that are now required in order to improve our understanding of how the HIS functions and how its malfunction may lead to hair follicle infection and hair growth disorders.

Note added in proof That the human HF is also a specialized immune compartment of the skin with a potentially critical role in immune surveillance has most recently been highlighted by the discovery that the distal ORS of human HF serves as an intermediate reservoir of Langerhans cells (Gilliam *et al*, 1998).

We are most grateful to Prof. W. Sterry for continued support and advice, and to R. Pliet and R. Böhmer for excellent technical assistance. This study was supported in part by grants from Deutsche Forschungsgemeinschaft (DFG Pa 345/3–2) and National Alopecia Areata Foundation to R.P.

REFERENCES

Allison JP, Havran WL: The immunobiology of T cells with invariant gamma delta antigen receptors. *Annu Rev Immunol* 9:679–705, 1991

Argyris TS: Hair growth induced by damage. *Adv Biol Skin* 9:339–345, 1967

Becker JC, Varki N, Bröcker EB, Reisfeld RA: Lymphocyte mediated alopecia in C57BL/6 mice following successful immunotherapy for melanoma. *J Invest Dermatol* 107:627–632, 1996

Bergstresser PR, Cruz PD Jr, Takashima A: Dendritic epidermal T cells: lessons from mice for humans. *J Invest Dermatol* 100:80S–83S, 1993

Billingham RE, Silvers WK: A biologists reflection on dermatology. *J Invest Dermatol* 57:495–499, 1971

Bos JD (ed.): *The Skin Immune System*. Boca Raton, CRC Press, 1997

Botchkarev VA, Paus R, Czarnetzki BM, Kupriyanov VS, Gordon DS, Johansson O: Hair cycle-dependent changes in mast cell histochemistry in murine skin. *Arch Dermatol Res* 287:683–686, 1995

Botchkarev VA, Eichmüller S, Peters EMJ, Pietsch P, Johansson O, Maurer M, Paus R: A simple immunofluorescence technique for simultaneous visualization of mast cells and nerve fibers reveals selectivity and hair cycle-dependent changes in mast cell-nerve fiber contacts in murine skin. *Arch Dermatol Res* 289:292–302, 1997

Cepek KL, Shaw SK, Parker CM, Russell GJ, Morrow JS, Rimm DL, Brenner MB: Adhesion between epithelial cells and T lymphocytes mediated by E-cadherin and the alpha E beta 7 integrin. *Nature* 372:190–193, 1994

Claesson MH, Hardt F: The influence of the hair follicle phase on the survival time of skin allografts in the mouse. *Transplantation* 10:349–351, 1970

Duraiswamy N, Tse Y, Hammerberg C, Kang S, Cooper KD: Distinction of class II MHC+ Langerhans cell-like interstitial dendritic antigen-presenting cells in murine dermis from dermal macrophages. *J Invest Dermatol* 103:678–683, 1994

Eichmüller S, Stevenson PA, Paus R: A new method for double immunolabelling with primary antibodies from identical species. *J Immunol Meth* 190:255–265, 1996

Elbe A, Tschachler E, Steiner G, Binder A, Wolff K, Stingl G: Maturational steps of bone marrow-derived dendritic murine epidermal cells. Phenotypic and functional studies on Langerhans cells and Thy-1+ dendritic epidermal cells in the perinatal period. *J Immunol* 143:2431–2438, 1989

Elbe A, Kilgus O, Strohal R, Payer E, Schreiber S, Stingl G: Fetal skin: a site of dendritic epidermal T cell development. *J Immunol* 149:1694–1701, 1992

Erle DJ: Intraepithelial lymphocytes. Scratching the surface. *Curr Biol* 5:252–254, 1995

Gilliam AC, Kremer IB, Yoshida Y, *et al*: The human hair follicle: A reservoir of $CD40^+$ B7-deficient Langerhans cells that regulate epidermis after UVB exposure. *J Invest Dermatol* 110:422–427, 1998

Goldsmith LA. (ed.): *Physiology, Biochemistry, and Molecular Biology of the Skin*. Oxford University of Press, New York, 1991

Goodman T, Lefrancois L: Intraepithelial lymphocytes. Anatomical site, not T cell receptor form, dictates phenotype and function. *J Exp Med* 170:1569–1581, 1989

Haas W, Pereira P, Tonegawa S: Gamma/delta cells. *Annu Rev Immunol* 11:637–685, 1993

Hamann K, Haas N, Grabbe J, Czarnetzki BM: Expression of stem cell factor in cutaneous mastocytosis. *Br J Dermatol* 133:203–208, 1995

Handjiski BK, Eichmüller S, Hofmann U, Czarnetzki BM, Paus R: Alkaline phosphatase activity and localization during the murine hair cycle. *Br J Dermatol* 131:303–310, 1994

Hardy MH: The secret life of the hair follicle. *Trends Genet* 8:55–61, 1992

Harrist TJ, Ruiter DJ, Mihm MC Jr, Bhan AK: Distribution of major histocompatibility antigens in normal skin. *Br J Dermatol* 109:623–633, 1983

Hashizume H, Tokura Y, Takigawa M: Increased number of dendritic epidermal T cells associated with induced anagen phase of hair cycles. *J Dermatol Sci* 8:119–124, 1994

Hirai Y, Nose A, Kobayashi S, Takeichi M: Expression and role of E- and P-cadherin adhesion molecules in embryonic histogenesis. II. Skin morphogenesis. *Development* 105:271–277, 1989

Hofmann U, Tokura Y, Nishijima T, Takigawa M, Paus R: Hair cycle dependent changes in skin immune functions: Anagen associated depression of sensitization for contact hypersensitivity in mice. *J Invest Dermatol* 106:598–604, 1996

Hofmann U, Tokura Y, Rückert R, Paus R: The anagen hair cycle induces systemic immunosuppression of contact hypersensitivity in mice. *Cellular Immunology.* in press, 1998.

Ikuta K, Weissman IL: Evidence that hematopoietic stem cells express mouse c-kit but do not depend on steel factor for their generation. *Proc Natl Acad Sci USA* 89:1502–1506, 1992

Janeway CA, Travers P: *Immunobiology.* Current Biology Ltd/Garland Publishing, London, 1997

Kilshaw PJ, Murant SJ: A new surface antigen on intraepithelial lymphocytes in the intestine. *Eur J Immunol* 20:2201–2207, 1990

Kraal G, Breel M, Janse M, Bruin G: Langerhans cells, veiled cells, and interdigitating cells in the mouse recognized by a monoclonal antibody. *J Exp Med* 163:981–997, 1986

Ledbetter JA, Rouse RV, Micklem HS, Herzenberg LA: T cell subsets defined by expression of Lyt-1,2,3 and Thy-1 antigens. Two-parameter immunofluorescence and cytotoxicity analysis with monoclonal antibodies modifies current views. *J Exp Med* 152:280–295, 1980

Lefrancois L, Barrett TA, Havran WL, Puddington L: Developmental expression of the alpha IEL beta 7 integrin on T cell receptor gamma delta and T cell receptor alpha beta T cells. *Eur J Immunol* 24:635–640, 1994

Maurer M, Paus R, Czarnetzki BM: Mast cells as modulators of hair follicle cycling. *Exp Dermatol* 4:266–271, 1995

Maurer M, Fischer E, Handjiski B, von Stebut E, Algermissen B, Bavandi A, Paus R: Activated skin mast cells are involved in murine hair follicle regression. *Lab Invest* 77:319–332, 1997

Melian A, Beckman EM, Porcelli SA, Brenner MB: Antigen presentation by CD1 and MHC-encoded class I-like molecules. *Curr Opin Immunol* 8:82–88, 1996

Nickoloff B (ed.): *Dermal Immune System*. CRC Press, Boca Raton, 1993

Noble WC (ed.): *The Skin Microflora and Microbial Disease*. Cambridge University Press, Cambridge, 1993

Parakkal PF: Role of macrophages in collagen resorption during hair growth cycle. *J Ultrastruct Res* 29:210–217, 1969

Paus R: Immunology of the hair follicle. In: Bos JD (ed.). *The Skin Immune System,* CRC Press, Boca Raton, 1997, pp. 377–398

Paus R, Stenn KS, Link RE: The induction of anagen hair growth in telogen mouse skin by cyclosporine A administration. *Lab Invest* 60:365–369, 1989

Paus R, Stenn KS, Link RE: Telogen skin contains an inhibitor of hair growth. *Br J Dermatol* 122:777–784, 1990

Paus R, Hofmann U, Eichmüller S, Czarnetzki BM: Distribution and changing density of gamma-delta T cells in murine skin during the induced hair cycle. *Br J Dermatol* 130:281–289, 1994a

Paus R, Eichmüller S, Hofmann U, Czarnetzki BM: Expression of classical and nonclassical MHC class I antigens in murine hair follicles. *Br J Dermatol* 131:177–183, 1994b

Paus R, Slominski A, Czarnetzki BM: Is alopecia areata an autoimmune-response against melanogenesis-related proteins, exposed by abnormal MHC class I-expression in the anagen hair bulb? *Yale J Biol Med* 66:541–554, 1994c

Paus R, Maurer M, Slominski A, Czarnetzki BM: Mast cell involvement in murine hair growth. *Dev Biol* 163:230–240, 1994d

Paus R, Handjiski B, Czarnetzki BM, Eichmüller S: A murine model for inducing and manipulating hair follicle regression (catagen): effects of dexamethasone and cyclosporin A. *J Invest Dermatol* 103:143–147, 1994e

Paus R, Handjiski B, Eichmüller S, Czarnetzki BM: Chemotherapy-induced alopecia in mice. Induction by cyclophosphamide, inhibition by cyclosporine A, and modulation by dexamethasone. *Am J Pathol* 144:719–734, 1994f

Paus R, Böttge JA, Henz BM, Maurer M: Hair growth control by immunosuppression. *Arch Dermatol Res* 288:408–410, 1996a

Paus R, Schilli MB, Handjiski B, Menrad A, Henz BM, Plonka P: Topical calcitriol enhances normal hair regrowth but does not prevent chemotherapy-induced alopecia in mice. *Cancer Res* 56:4438–4443, 1996b

Paus R, Foitzik K, Welker P, Bulfone-Paus S, Eichmüller S: Transforming growth factor-beta receptor type I and type II expression during murine hair follicle development and cycling. *J Invest Dermatol* 109:518–526, 1997

Payer E, Elbe A, Stingl G: Circulating CD3+/T cell receptor Vγ3+ fetal murine thymocytes home to the skin and give rise to proliferating dendritic epidermal T cells. *J Immunol* 146:2536–2543, 1991

Porcelli S, Brenner MB, Greenstein JL, Balk SP, Terhorst C, Bleicher PA: Recognition of cluster of differentiation 1 antigens by human CD4-CD8-cytolytic T lymphocytes. *Nature* 341:447–450, 1989

Rötzschke O, Falk K, Stevanovic S, Grahovac B, Soloski MJ, Jung G, Rammensee HG: Qa-2 molecules are peptide receptors of higher stringency than ordinary class I molecules. *Nature* 361:642–644, 1993

Roulston A, Lin R, Beauparlant P, Wainberg MA, Hiscott J: Regulation of human immunodeficiency virus type 1 and cytokine gene expression in myeloid cells by NF-kappa B/Rel transcription factors. *Microbiol Rev* 59:481–505, 1995

Rückert R, Hofmann U, van der Veen C, Bulfone-Paus S, Paus R: MHC class I expression in murine skin: developmentally controlled and strikingly restricted intraepithelial expression during hair follicle morphogenesis and cycling, and response to cytokine treatment *in vivo*. *J Invest Dermatol* 111:25–30, 1998

Schuler G (ed.): *Epidermal Langerhans Cells*. CRC Press, Boca Raton, 1991

Shawar SM, Vyas JM, Rodgers JR, Rich RR: Antigen presentation by major histocompatibility complex class I-B molecules. *Annu Rev Immunol* 12:839–880, 1994

Slominski A, Goodman-Snitkoff G, Maurer M, Paus R: Hair cycle-associated changes in splenocyte proliferation. *In Vivo* 11:101–102, 1997

Springer T, Galfre G, Secher DS, Milstein C: Mac-1: a macrophage differentiation antigen identified by monoclonal antibody. *Eur J Immunol* 9:301–306, 1979

Tamaki K, Yasaka N, Chang CH, Ohtake N, Saitoh A, Nakamura K, Furue M: Identification and characterization of novel dermal Thy-1 antigen-bearing dendritic cells in murine skin. *J Invest Dermatol* 106:571–575, 1996

Tigelaar RE, Lewis JM: Immunobiology of mouse dendritic epidermal T cells: a decade later, some answers, but still more questions. *J Invest Dermatol* 105:43S–49S, 1995

Tigelaar RE, Lewis JM, Nixon-Fulton JL, Bergstresser PR: Thy-1 antigen-bearing dendritic epidermal cells in mice. In: LA Goldsmith (ed.). *Physiology, Biochemistry, and Molecular Biology of the Skin*. Oxford University Press, New York, 1991, pp. 1164–1186

Tokura Y, Hofmann U, Müller-Röver S, *et al*: Spontaneous hair follicle cycling may influence the development of murine contact photosensitivity by modulating keratinocyte cytokine production. *Cell Immunol* 178:172–179, 1997

Vielkind U, Sebzda MK, Gibson IR, Hardy MH: Dynamics of Merkel cell patterns in developing hair follicles in the dorsal skin of mice, demonstrated by a monoclonal antibody to mouse keratin 8. *Acta Anat* 152:93–109, 1995

van Vliet E, Melis M, van Ewijk W: Monoclonal antibodies to stromal cell types of the mouse thymus. *Eur J Immunol* 14:524–529, 1984

Wallgren AC, Karlsson Parra A, Korsgren O: The main infiltrating cell in xenograft rejection is a CD4+ macrophage and not a T lymphocyte. *Transplantation* 60:594–601, 1995

Westgate GE, Craggs RI, Gibson WT: Immune privilege in hair growth. *J Invest Dermatol* 97:417–420, 1991

Yoshida-Noro C, Suzuki N, Takeichi M: Molecular nature of the calcium-dependent cell-cell adhesion system in mouse teratocarcinoma and embryonic cells studied with a monoclonal antibody. *Dev Biol* 101:19–27, 1984